The impact of gradational contact at the reservoir-seal interface on geological CO2 storage capacity and security

Onoja, M & Shariatipour, SM

Author post-print (accepted) deposited by Coventry University's Repository

Original citation & hyperlink:
Onoja, M & Shariatipour, SM 2018, 'The impact of gradational contact at the reservoir-seal interface on geological CO2 storage capacity and security' *International Journal of Greenhouse Gas Control*, vol 72, pp. 1-13
https://dx.doi.org/10.1016/J.IJGGC.2018.03.007

DOI 10.1016/J.IJGGC.2018.03.007
ISSN 1750-5836

Publisher: Elsevier

NOTICE: this is the author's version of a work that was accepted for publication in *International Journal of Greenhouse Gas Control*. Changes resulting from the publishing process, such as peer review, editing, corrections, structural formatting, and other quality control mechanisms may not be reflected in this document. Changes may have been made to this work since it was submitted for publication. A definitive version was subsequently published in *International Journal of Greenhouse Gas Control*, [72, (2018)] DOI: 10.1016/J.IJGGC.2018.03.007

© 2018, Elsevier. Licensed under the Creative Commons Attribution-NonCommercial-NoDerivatives 4.0 International
http://creativecommons.org/licenses/by-nc-nd/4.0/

Copyright © and Moral Rights are retained by the author(s) and/ or other copyright owners. A copy can be downloaded for personal non-commercial research or study, without prior permission or charge. This item cannot be reproduced or quoted extensively from without first obtaining permission in writing from the copyright holder(s). The content must not be changed in any way or sold commercially in any format or medium without the formal permission of the copyright holders.

This document is the author's post-print version, incorporating any revisions agreed during the peer-review process. Some differences between the published version and this version may remain and you are advised to consult the published version if you wish to cite from it.

The Impact of Gradational Contact at the Reservoir-Seal Interface on Geological CO_2 Storage Capacity and Security

Michael U. Onoja[a*], Seyed M. Shariatipour[a]

[a] Centre for Flow Measurement and Fluid Mechanics, Maudslay House, Coventry University. CV1 2NL. Coventry, United Kingdom.

* Corresponding author: onojau@coventry.ac.uk

ACCEPTED MANUSCRIPT

Abstract

The implementation of CO_2 storage in sub-surface sedimentary formations can involve decision making using relevant numerical modelling. These models are often represented by 2D or 3D grids that show an abrupt boundary between the reservoir and the seal lithologies. However, in an actual geological formation, an abrupt contact does not always exist at the interface between distinct clastic lithologies such as sandstone and shale. This article presents a numerical investigation of the effect of sediment-size variation on CO_2 transport processes in saline aquifers. Using the Triassic Bunter Sandstone Formation (BSF) of the Southern North Sea (SNS), this study investigates the impact a gradation change at the reservoir-seal interface on CO_2 sequestration. This is of great interest due to the importance of enhanced geological detail in reservoir models used to predict CO_2 plume migration and the integrity of trapping mechanisms within the storage formation. The simplified strategy was to apply the *Van Genutchen* formulation to establish constitutive relationships for pore geometric properties, which include capillary pressure (P_c) and relative permeability (k_r), as a function of brine saturation in the porous media. The results show that the existence of sediment gradation at the reservoir-seal interface and within the reservoir has an important effect on CO_2 migration and pressure diffusion in the formation. The modelling exercise shows that these features can lead to an increase in residual gas trapping in the reservoir and localised pore pressures at the caprock's injection point.

Keywords:

CO_2 Sequestration; Capillary Pressure; Relative Permeability; Physical Trapping; Clastic Sediments.

ACCEPTED MANUSCRIPT

1. Introduction

The geological storage of carbon dioxide (CO_2) serves as an option to sequester CO_2 emissions from the atmosphere. Carbon Capture and Storage (CCS) is a three-step process that involves CO_2 capture, its transport, and subsequent underground storage. It was inspired by the utilisation of CO_2 in enhanced oil or gas recovery (EOR or EGR) which offers potential economic gain from the increased production of hydrocarbons (Bondor, 1992; Martin and Taber, 1992; Kovscek and Cakici, 2005; Grigg, 2005; Gozalpour *et al.*, 2005). Various studies on this approach, duly summarised in the Intergovernmental Panel on Climate Change (IPCC) special report on carbon capture and storage, have elaborated on the feasibility of mitigating the adverse effects of this greenhouse gas while enhancing the recovery of fossil fuels for future energy production (IPCC, 2005). The report outlines sedimentary rocks as naturally ideal media for geologic CO_2 sequestration (GCS), and deep saline aquifers as subsurface formations which possess the largest storage capacity. One critical issue in GCS, however, is demonstrating the long-term safety and security of subsurface CO_2 storage. This entails assessing the potential for CO_2 leakage from deep formations into shallow groundwater aquifer zones (Zheng *et al.*, 2013; Lawter *et al.*, 2017) as well as any possibility of injection-induced seismicity (Nicol *et al., 2011;* Dempsey *et al.*, 2014). Undoubtedly, this has necessitated a broad scientific approach that elucidates the geological processes influencing the estimation of CO_2 storage capacity and the integrity of caprocks overlying the storage aquifers (Bachu, 2015). This approach usually involves the use of numerical models which incorporate reservoir parameters such as porosity, permeability, and saturation functions to solve the governing equations for subsurface fluid flow and transport. The models simulate complex geological processes which aid in the design of injection schemes as well as the assessment of storage capacities in target locations.

In petroleum literature, numerical models are commonly applied to the quantitative analysis of heterogeneic effects in subsurface storage media (e.g. Pruess *et al.*, 2003; Doughty and Pruess, 2004; Kumar *et al.*, 2005; Mo *et al*., 2005). A number of studies using numerical models acknowledge the importance of two constitutive functions: capillary pressure (P_c) and relative permeability (k_r), on multiphase fluid flow during GCS (Fleet *et al.*, 2004; Ennis-King and Paterson, 2005; Juanes *et al.*, 2006; Obi and Blunt, 2006; Burton *et al.*, 2009; Kopp *et al.*, 2009). The main aim of this study is to

ACCEPTED MANUSCRIPT

investigate the variability in transport and flow processes of injected CO_2 resulting from a gradational contact at the reservoir-seal interface and the gradual change in clast-size within an aquifer. This variability is described in consitutive functions using an empirical correlation that is based on grain-size variation i.e Van Genuchten's (1980) formulation. Through this contribution, we intend to encourage the representation of heterogeneity in capillary pressure (P_c) and relative permeability (k_r) functions during reservoir simulation. To the best of our knowledge, no large-scale study on GCS has incorporated such small-scale variability in both P_c– and k_r–saturation curves. Although Saadatpoor *et al.* (2010) and Meckel *et al.* (2015) showed the influence of grain-scale heterogeneity on a reservoir-scale, their studies only emphasised the influence of capillary heterogeneity on CO_2 storage performance. The former scaled the variability flow processes using intrinsic permeability heterogeneity with a spatially constant capillary pressure curve, while the latter introduced capillary heterogeneity by generating a capillary threshold pressure distribution based on defined median grain size. In this study, we scale capillary heterogeneity from a spatially constant threshold pressure and describe variation in relative permeability curves through the grain size. The contribution of other effects such as the wettability of the porous medium and the interfacial tension between the fluids in contact are not considered here.

2. Problem statement

Reservoir heterogeneity is dominated by depositional and diagenetic processes. The sedimentology of the formation primarily influences the reservoir quality by regulating its pore system (Pettijohn *et al.*, 1972). This dictates the porosity and permeability of the media and in turn controls the storage capacity and the efficiency of physical trapping mechanisms during CO_2 sequestration (Benson and Cole, 2008). The physical and chemical changes that alter the characteristics of sediments after deposition are reffered to as diagenesis. Volumetrically, siliciclastic rocks are the most important variety of sedimentary rocks for GCS (Boggs, 2009). Clasts, i.e. rock fragments, vary in size ranging from fine-textured clay and silt, to medium-textured sand (see Table 1), up to coarse-textured pebble, cobble and boulder sized materials (Wentworth, 1922). During transportation and deposition, the clasts are sorted according to their average grain-size diameter and deposited in a geological sequence of interleaved rocks known sedimentary beds or strata (Hiscott, 2003). Consequently,

ACCEPTED MANUSCRIPT

sedimentary structures such as gradational contacts or graded beds are formed. Gradational contact describes the gradual transition in the average size of deposited clasts between conformable strata while graded bedding refers to the vertical evolution of grain size in a stratum. These structures are reservoir-scale heterogeneities which can influence injected CO_2 flow patterns due to distinct hydraulic conductivities arising from grain-scale heterogeneities. Grain-scale heterogeneity dictates the capillary effect that governs two physical traps: stratigraphic and residual gas trapping (Bjørlykke, 2010). This capillarity effect emanates from fluid and interfacial physics at the pore-scale. Hence, the effective hydraulic behaviour on any practical field-scale is dominated by the large scale spatial-arrangement of small-scale variability (Krevor *et al.,* 2015). The reader is referred to Pettijohn (1957) and Haldorsen (1986) for the basics of sedimentary structures and scales of heterogeneity, respectively.

<table>
<tr><th>Geological Size Range (mm)</th><th>Sediment Texture</th><th colspan="2">General term for Consolidated Rock</th></tr>
<tr><td>2.0 - 1.0</td><td>Very coarse sand</td><td colspan="2" rowspan="5">Sandstone</td></tr>
<tr><td>1.0 - 0.5</td><td>Coarse sand</td></tr>
<tr><td>0.5 - 0.25</td><td>Medium sand</td></tr>
<tr><td>0.25 - 0.125</td><td>Fine sand</td></tr>
<tr><td>0.125 - 0.0625</td><td>Very fine sand</td></tr>
<tr><td>0.0625 - 0.0313</td><td>Coarse silt</td><td rowspan="4">Siltstone</td><td rowspan="5">Mudstone (Shale)</td></tr>
<tr><td>0.0313 - 0.0156</td><td>Medium silt</td></tr>
<tr><td>0.0156 - 0.0078</td><td>Fine silt</td></tr>
<tr><td>0.0078 - 0.0039</td><td>Very fine silt</td></tr>
<tr><td>< 0.0039</td><td>Clay</td><td>Claystone</td></tr>
</table>

Table 1: The Wentworth scale for clastic sediments (Wentworth, 1922)

2.1 The reservoir-seal interface

The lithostratigraphic units of many generic reservoir models are usually interpreted from wireline logs of representative geologies, such as the Gamma Ray (GR) tool (Doveton, 1991; Darling, 2005). However, the GR log may be considered to fall short of its capabilities when distinguishing between types of mudstones, i.e. siltstone and claystone. This is because the primary radioactive isotopes in rocks, i.e. potassium, thorium and uranium, are more common in clay minerals than in sand and silt (Bigelow, 1992), hence the GR log is often used as a measure of shale content (Katahara, 1995; Fabricius *et al.*, 2003; Nazeer *et al.*, 2016). Since clay distribution

ACCEPTED MANUSCRIPT

alone cannot account for the fine-grained sediments in an actual reservoir, it is important to assess the impact of sediment-size gradation on GCS, particularly at the reservoir-seal interface. Most models that simulate CO_2 plume distribution are built under the assumption that the stratigraphic contact between the reservoir rock and the caprock is abrupt (i.e. a sudden distinctive change in the lithology). This may not always be the case in geological formations because the bedding contact between sandstone and mudstone can show a gradation in particle sizes at the interface. For example, the Sherwood Sandstone Group shows an upward grading of sediments from coarse sandstones to siltstones, and then to the Mercia Mudstone Group (Benton *et al.*, 2002; Newell 2017). Nevertheless, a number of contemporary studies performed using reservoir models have included geological details such as top-surface morphologies and transition zone heterogeneities (e.g. Shariatipour *et al.*, 2014; 2016; Newell and Shariatipour, 2016). These studies demonstrated that such geological detail can affect various trapping mechanisms within the reservoir as well as influence CO_2 plume migration, the estimation of storage capacity, and the volume of the aquifer. Generally, increasing the level of detail in geological modeling for simulation models is essential for producing meaningful and accurate results (Van De Graaff and Ealey, 1989).

2.2 Describing flow characteristics in reservoir models

Due to the scarcity of experimental data on P_c and k_r, the common practice in reservoir modelling is the use of empirical formulations to describe flow characteristics. Many GCS studies have adopted the constitutive functions by either Brooks and Corey (1966) or Van Genuchten (1980) to describe the capillary pressure (P_c), saturation (S), and relative permeability (k_r) relationship (P_c–S–k_r relationship) in the flow model (e.g. Class *et al.*, 2009; Oldenburg *et al.*, 2001; Cameron and Durlofsky, 2012). A comprehensive review by Oostrom *et al.* (2016) highlights the van Genuchten, *VG*, function to be much more efficient in describing the dynamic fluid model in GCS. This is usually coupled to Mualem's (1976) and Corey's (1954) formulations to give the integrated Van Genutchten-Mualem-Corey (VGMC) flow model for P_c–S–k_r relationships:

$$S_w + S_{nw} = 1 \tag{1}$$

$$S_{ew} = \frac{S_w - S_{w,min}}{S_{w,max} - S_{w,min}} \tag{2}$$

ACCEPTED MANUSCRIPT

$$P_c = P_e\left[(S_{ew})^{-\frac{1}{m}} - 1\right]^{\frac{1}{m}} \qquad (3)$$

$$k_{rw} = (S_{ew})^{\frac{1}{2}}\left[1 - \left(1 - (S_{ew})^{1/m}\right)^{m}\right]^2 \qquad (4)$$

$$k_{rnw} = (1 - S_{ew})^2\,(1 - (S_{ew})^2) \qquad (5)$$

where S_{ew} is the effective wetting fluid saturation; $S_{w,min}$ and $S_{w,max}$ represent the minimum and maximum saturation for the wetting fluid which occurs for a given problem at an actual wetting fluid saturation of S_w; S_{nw} is the saturation of the non-wetting fluid; P_e is the capillary entry pressure; k_{rw} and k_{rnw} are relative permeability values for the wetting fluid and the non-wetting fluid respectively, at an effective wetting fluid saturation, S_{ew}; n and m correspond to pore geometry/model parameters related by the assumption that $m = 1 - {}^{1}/_{n}$.

A large number of numerical models that have used this flow model assumed a generic parameter value of 0.457 for the pore size index, m (Oostrom *et al.*, 2016). According to Birkholzer *et al.* (2009) this value is typical of sedimentary formations suitable for CO_2 storage. A vast number of studies have used a constant value for the fitting parameter, m, to generate P_c–S–k_r relationships irrespective of the geological heterogeneity of the model (e.g. Gor *et al.*, 2013; Zhou *et al.*, 2010; Al-Khdheeawi *et al.*, 2017; Espinet *et al.*, 2013). Utilising a fixed value to represent the pore size distribution index of an entire storage formation fails to account for the differences in the average pore size of rock lithologies within strata in the reservoir. Additionally, predictions from such reservoir models may fall short of precision because the accuracy of flow processes in a porous medium is highly dependent on the description of the P_c–S–k_r relationship (Mori *et al.*, 2015).

3. Methodology

In this paper, we employ Carsel and Parrish's (1988) descriptive statistics for the pore size distribution index, n, and introduce a parameterisation scheme that describes the fluid flow behaviour of various clastic rocks (Table 2):

General term for consolidated rock	**Sedimentary components (%)**			**Van Genuchten Parameter (n)**	**Term for Consolidated Rock as used in this study**
	Sand	**Silt**	**Clay**		

ACCEPTED MANUSCRIPT

Sandstone	> 85	Silt + (1.5*Clay) < 15		2.68	Coarse Sandstone
Sandstone	70 – 90	Silt + (1.5*Clay) ≥ 15; and Silt + (2*Clay) < 30		2.28	Sandstone
Sandstone	> 52	Silt + (2*Clay) ≥ 30; if a) Clay is between 7 – 20, or b) Clay < 7, and Silt < 50		1.89	Silty Sandstone
Sandstone	< 52	28 - 50	7 - 27	1.56	Muddy Sandstone
Sandstone	> 45	< 28	20 - 35	1.48	Clayey Sandstone
Mudstone	20 – 50	50 - 80	12 - 27	1.41	Sandy Siltstone
Mudstone	< 20	> 80	< 12	1.37	Siltstone
Mudstone	< 45	< 40	> 40	1.09	Claystone

Table 2: Sedimentary components and the terminology for clastic sedimentary rocks (USDA, 1987; Folk, 1974), along with the associated *VG* parameter from Carsel and Parrish (1988).

3.1. Model Development

The study is patterned after the Triassic Bunter Sandstone Formation (BSF) of the Southern North Sea (SNS) in the United Kingdom (UK) sector (Williams *et al.*, 2013). The BSF is a reservoir unit composed of predominantly medium- to coarse-grained sandstone units of metre-scale upward coarsening regime interbedded with fine-grained sediments (Rhys, 1974). It is described as the major gas producing reservoir in the SNS. Most of the BSF is filled with saline water and considered to have significant CO_2 storage potential. In the UK sector, it overlies the Triassic Bunter shale formation and is sealed by mudstones and evaporites of the upper Triassic Haisborugh Group (Brook *et al.*, 2003). Structurally, Bunter sandstones contain several periclines commonly referred to as Bunter domes (Williams *et al.*, 2013). Based on previous investigations and studies, one such Bunter dome in the UK sector was recently identified by the Energy Technologies Institute's UK CO_2 Storage Appraisal Project (UKSAP) as a promising candidate for CO_2 storage (James et al., 2016). This dome is penetrated by Well 44/26-01, a deep exploration well completed in 1968 with interpreted log data identifying the strata within the dome (see Fig. 1).

The BSF within this dome is interpreted as having five intra-reservoir sandstone zones possessing interbedded shale and cemented sandstone layers. A detailed description of the sedimentology and lithostratigraphy of this dome, hereafter referred to as *Bunter aquifer*, was given by Williams *et al*. (2013). Here we present only a brief overview of Bunter aquifer in order to justify the lithological modelling approach used to

ACCEPTED MANUSCRIPT

investigate the multiphase fluid flow regime resulting from pore scale variation in the reservoir-seal interface. The reservoir-seal interface is assumed to be Zone 1 (Fig. 1) and henceforth referred to as the *transition zone*. Because this is a generic study of CO_2 storage in deep sandstone aquifers overlain by mudstones, rather than the study of a specific aquifer, the goal was to select representative characteristics for the aquifer as a base case for systematic parameter study. As such, the thickness and other aquifer characteristics were based on the log data from Well 44/26-01.

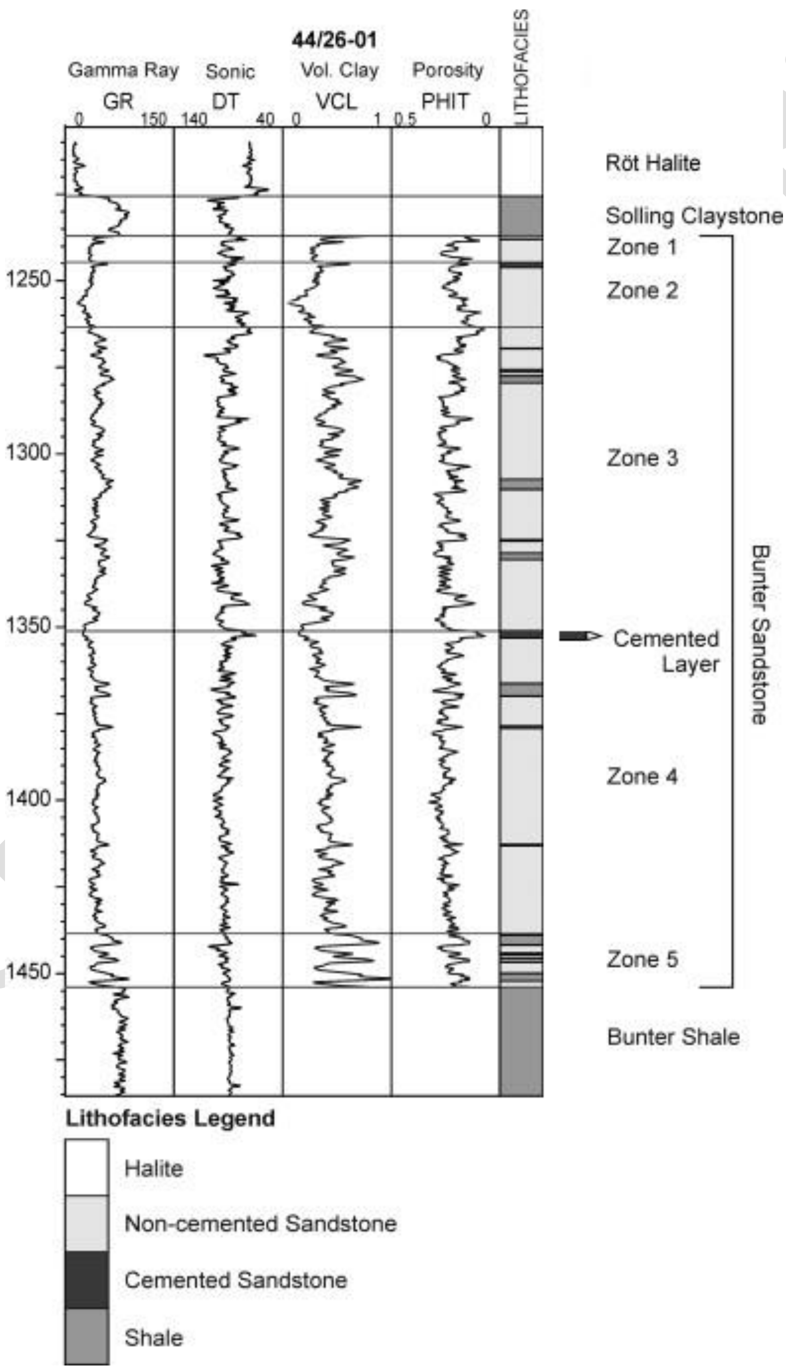

Fig. 1: Lithostratighraphical correlation of Bunter Well 44/26-01 from logging data (Williams *et al.*, 2013).

3.2 Numerical Modelling

A simplified 3D static geological model with an areal size of 2 km x 2 km and a thickness of 300 m was developed and discretised into a total of 544,000 active cells (n_i = 80, n_j = 80, n_k = 85) using Schlumberger's PETREL software (Schlumberger, 2016). Although the study is based on a dome-like structure, the geological layering in this model is horizontal (Fig. 2).

Zones	Top depth (m)	Number of layers
Rot Halite	1200	4
Claystone	1225	12
R.Zone 1	1237	8
R.Zone 2	1245	10
R.Zone 3	1264	15
R.Zone 4	1350	22
R.Zone 5	1438	5
Base Shale	1455	9

Table 3: Vertical grid discretisation for the modelling domain.

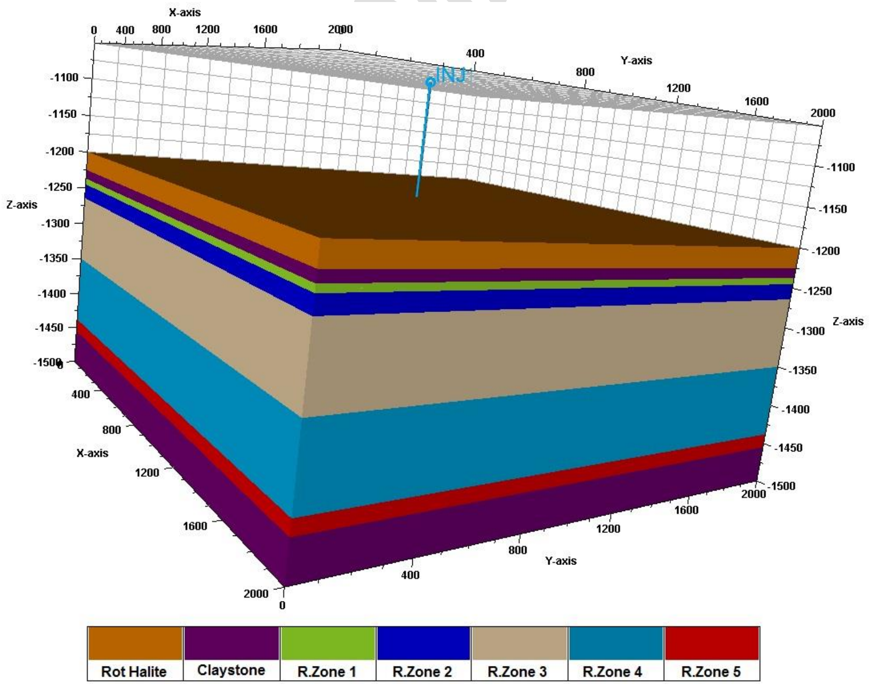

Fig. 2: Reservoir model used for ECLIPSE simulations.

An average horizontal permeability (K_h) value of 6.5 x 10^{-3} mD was assigned to the top and base seal lithologies, after Spain and Conrad (1997), while the average K_h for

ACCEPTED MANUSCRIPT

the reservoir was assumed to be 233 mD. The top seal capacities of the Solling Claystone and the Rot Halite were assigned porosity values of 4% and 1% respectively. This was based on the range of porosity values in the Solling, Rot, and Muschelkalk caprocks above the BSF in the southern Dutch North Sea (Spain and Conrad, 1997). The base seal and reservoir formation in the model were assigned average porosity values of 4% and 22% respectively. Permeability anisotropy was assumed to be 0.3 since the average vertical permeabilities of the Bunter sandstone are reported to be typically some 30 % lower than the horizontal permeabilities (Noy *et al.*, 2012). Pore fluid in the domain was modelled under an isothermal condition of 42°C and an initial pressure of 12 MPa with a brine pore fluid gradient of 10.7 MPa/km. This implies a pore fluid density of 1.09 g/cc at a salinity of 133,000 ppm. Pressure control consideration for dynamic modelling is 75% of a lithostatic pressure gradient of 22.5 MPa/km (after Noy *et al.*, 2012).

P_c-S-k_r relationships were generated under the assumption of a strongly water wet system with a CO_2/brine interfacial tension of 30 mN/m, following published results by Hebach *et al.* (2002), Chiquet *et al.* (2007), and Perrin and Benson (2010). Draining and imbibition curves were included allowing for the residual trapping of CO_2 to be modelled (Fig 3):

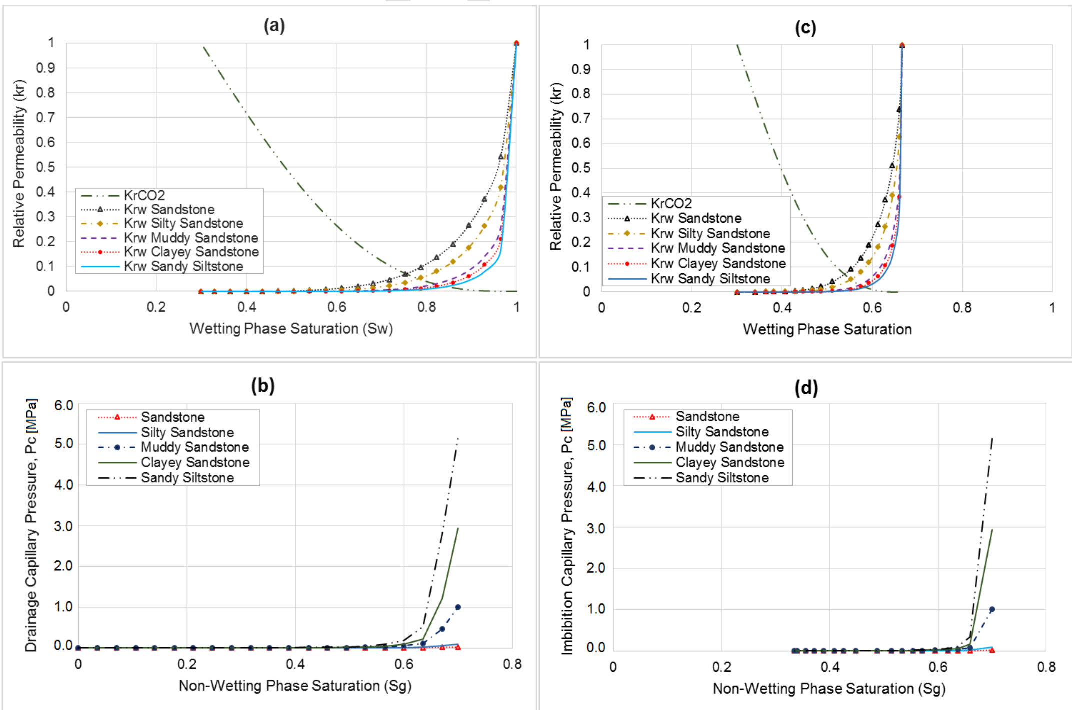

Fig. 3: P_c-S-k_r functions for (a) drainage relative permeability, (b) drainage capillary pressure, (c) imbibition relative permeability, and (d) imbibition capillary pressure

ACCEPTED MANUSCRIPT

CO_2 saturation end points for the reservoir and seal were based on published results for the Captain formation in the North Sea Goldeneye Field (Shell, 2011) and the Colorado Shale (Bennion and Bachu, 2008) respectively. The capillary displacement pressure of shale was assumed to be 4.7 MPa after Spain and Conrad's (1997) experimental investigation on the Solling Claystone in the southern Dutch North Sea. In the absence of closely related data, the maximum pore throat size in the reservoir was assumed to be 37 microns. This value falls within the range of dominant pore throat sizes of Permo-Triassic sandstones in the United Kingdom (Bloomfield *et al.*, 2001). Numerical simulations were conducted using ECLIPSE E300 (Schlumberger, 2015) which adopts Darcy's law description for immiscible two-phase flows in porous media (Bear, 1972). This study assumes no conductive faults, nor cemented sand layers, interbedded shale or leaky wellbores in the formation.

3.3 Sensitivity Design

Simulation studies were conducted in aquifer systems idealised as "closed" and "open" to observe the impact of the two sedimentary structures identified in Section 1 on CO_2 storage. The closed aquifer system was identified as Aquifer-1 while the open aquifer system was identified as Aquifer-2. The concept of graded bedding was investigated using normal grading where the strata coarsens downwards, and inverse grading where the strata coarsens upwards. Five reservoir lithologies were identified from Table 2. In the order of decreasing particle size, these reservoir lithologies are sandstone, silty sandstone, muddy sandstone, clayey sandstone, and sandy siltstone, respectively. The spatial porosity value of 22% remained the same for all the reservoir lithologies. However, permeability data for the varying lithologies were extrapolated from rock permeability values used in UKSAP's 2016 report for the intra-reservoir zones (James *et al.*, 2016):

Rock lithology	**Rock permeability [mD]**
Sandstone (S)	233
Silty Sandstone (SiS)	223
Muddy Sandstone (MS)	219
Clayey Sandstone (CS)	195
Sandy Siltstone (SSi)	162

Table 4: Permeability data for reservoir rock lithologies

The plot of the sensitivity study was outlined in three phases:

ACCEPTED MANUSCRIPT

- ***Phase I*** focused on the effect of varying the dynamic properties of the rock geometry (i.e. the P_c–S–k_r functions) in the reservoir model at a constant permeability within the reservoir.
- ***Phase II*** focused on the effect of varying the permeability values and the P_c–S–k_r functions in the reservoir. Simulation cases in this phase were identified by the suffix “A”.
- ***Phase III*** cases, identified by the suffix “B”, were modelled with variable permeability values and a single P_c–S–k_r function within the reservoir. This was to compare, in magnitude, the “stand-alone” effect of P_c–S–k_r functions over intrinsic permeability functions in the modelled domain.

For this study, permeability and porosity data are henceforth regarded as *the static functions* while P_c–S–k_r functions are regarded as *the dynamic functions*. The base case for the simulation regarded all five reservoir zones as sandstone and was identified as CASE 1. Sensitivity cases were then labelled according to the description in Table 5:

<table>
<tr><th>Reservoir Zone / Case</th><th>1</th><th>2</th><th>3</th><th>4</th><th>5</th></tr>
<tr><td>1</td><td>Sandstone</td><td>Sandstone</td><td>Sandstone</td><td>Sandstone</td><td>Sandstone</td></tr>
<tr><td>2</td><td>Sandstone</td><td>Silty Sandstone</td><td>Muddy Sandstone</td><td>Clayey Sandstone</td><td>Sandy Siltstone</td></tr>
<tr><td>3</td><td>Sandy Siltstone</td><td>Clayey Sandstone</td><td>Muddy Sandstone</td><td>Silty Sandstone</td><td>Sandstone</td></tr>
<tr><td>4</td><td>Silty Sandstone</td><td colspan="4" rowspan="4">Sandstone</td></tr>
<tr><td>5</td><td>Muddy Sandstone</td></tr>
<tr><td>6</td><td>Clayey Sandstone</td></tr>
<tr><td>7</td><td>Sandy Siltstone</td></tr>
</table>

Table 5: Pore geometric parameters for the reservoir simulation.

3.3.1 Aquifer-1

Aquifer-1 was confined vertically and laterally within the modelled domain (Fig 2) and had a reservoir pore volume of 1.93 x 10^8 m^3. This aquifer was used to investigate the impact of gradational contact and graded bedding on the reservoir’s injectivity and

ACCEPTED MANUSCRIPT

physical trapping mechanisms. In this aquifer, a numerical simulation was initiated at an annual CO_2 injection rate of 100,000 metric tonnes through an injection well peforated in R.Zone 4 and 5. The sensitivity plots of Phase I, II and III were investigated in this aquifer.

3.3.2 Aquifer-2

Aquifer-2 was confined in the vertical boundaries of the modelled domain but was assumed to have lateral aquifer connection. This aquifer was used to investigate the impact of gradational contact and graded bedding on overpressure at the reservoir-seal interface. The concept of an open aquifer was introduced in the study because closed aquifers do not communicate with other reservoirs, laterally, and as a result, may be under- or over-pressured following the CO_2 injection (Elewaut *et al.*, 1996). For two-phase flow in porous media, one important role the aqueous phase plays in affecting the evolution of CO_2 plume is that it serves as a pressure transmission medium within the porous media (Pruess and Nordbotten, 2011). As a result, the ease with which the migrating CO_2 plume evacuates brine from the pore space will influence the pressure evolution within the formation.

4. Results and Discussion

4.1 Reservoir Injectivity

For the simulation of gas injection, CO_2 plume was observed to rise vertically to the superjacent impermeable barrier. This buoyant migration of the plume was due to the density difference between the supercritical CO_2 and brine. Simulation results for reservoir injectivity for all three phases of the analysis showed an equivalence in CO_2 injection with time for the first 13 years of injection before reaching the limiting field pressure in the 14^{th} year of injection (Fig. 4):

ACCEPTED MANUSCRIPT

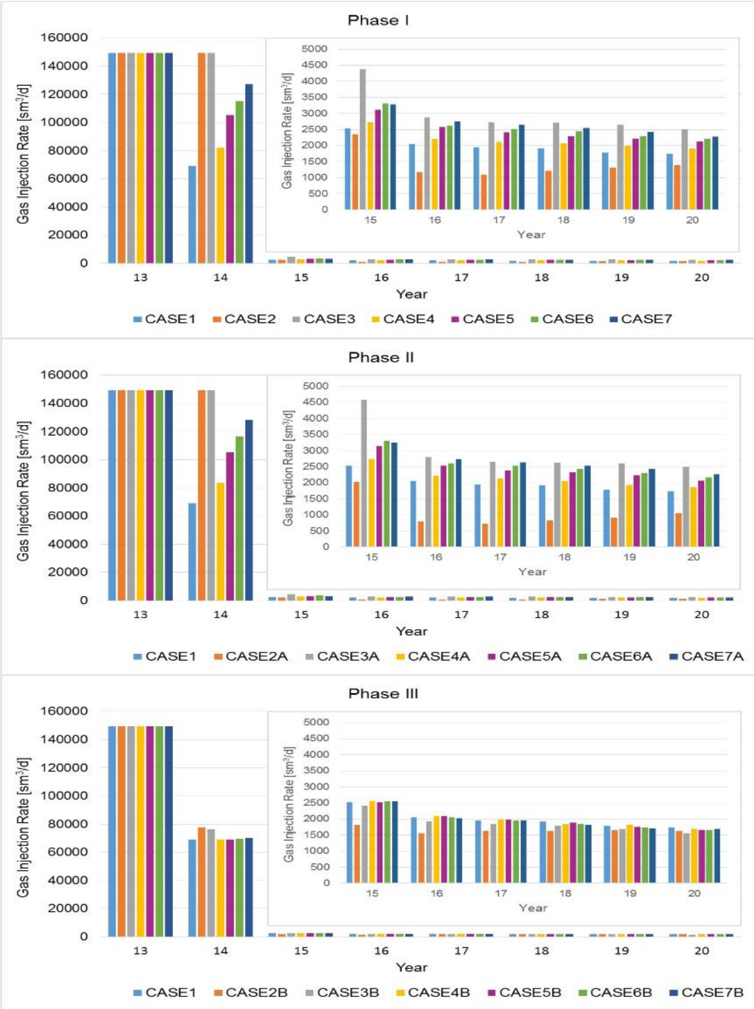

Fig. 4: CO_2 injection rates for all sensitivity cases.

The illustrations in Fig. 4 show the importance of the P_c–S–k_r functions on a reservoir's injectivity. Incorporating this dynamic relationship for heterogeneity at the transition zone was a major influence on the reservoir injectivity as the pore fluid pressure approached the well control pressure. For gradational contact at the reservoir-seal interface, the rate of CO_2 injection into the lower part of the reservoir increases with the decrease in size of clastic sediments at the top of the reservoir. For the graded reservoir, the rate of CO_2 injection favors normal grading over reverse grading. This can be seen from the 14th year of injection. The results indicate that the relative permeability functions predominate over permeability and porosity data when describing sedimentary heterogeneity. This is further emphasised in the comparison between the total CO_2 injected for all cases investigated. Fig. 5 shows neglible differences in the total amount of CO_2 injected between the base case and other sensitivity cases at the end of simulation for Phase III as opposed to Phases I and II:

ACCEPTED MANUSCRIPT

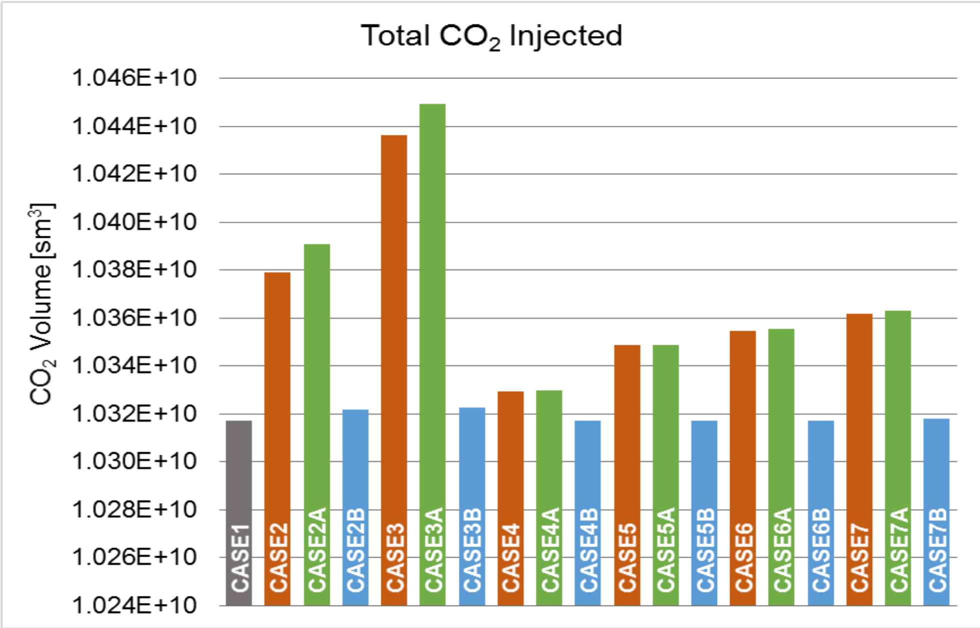

Fig. 5: Total volume of CO_2 injected into the reservoir during Phase III analysis

At the end of the simulation, all cases that used the P_c–S–k_r functions to describe hetergeneity within the model allowed for more CO_2 injection than the base case. In Fig. 5, Cases 4 and 4A show the smallest margin in total CO_2 injection and this accounts for an additional 23,000 tonnes of CO_2 being injected into the reservoir.

4.2 Physical Trapping

At the end of the injection period, the upward migration of CO_2 plume was restrained by the caprock layer in all the cases simulated. When graded bedding was incorporated into the pore geometric analysis, the impact of the dynamic functions followed the trend identified in Section 4.1 and amplified the supporting role of the static parameter thereby decreasing the effective permeability to the non-wetting phase. This was attributed to the impact of the irreducible aqueous phase on the relative permeability to CO_2 within the reservoir. Fig. 6 illustrates this impact based on the *VGMC*-model (section 2.2) which described a constant K_{rCO2}-S curve for all the reservoir lithologies in this study:

ACCEPTED MANUSCRIPT

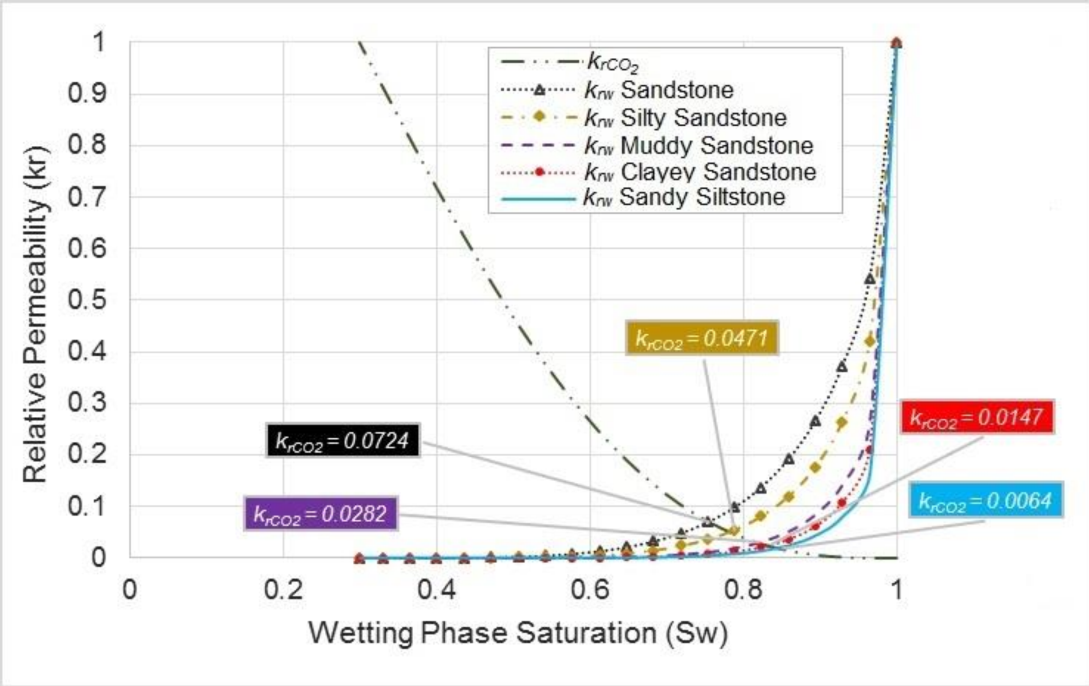

Fig. 6: Relative permeability curves showing the value for $k_{r(CO2)}$ at the intercept of $k_{r(brine)}$ in various reservoir lithologies

Fig. 6 shows a decreasing value of the relative permeability to CO_2 at the intercept between the non-wetting k_{rnw}-S curve and the variable wetting k_{rw}-S curves for the reservoir rocks. This resulted in a lower degree of mobile CO_2 in models that incorporated smaller clasts within the reservoir, particularly at the transition zone. The relative drag in plume movement within the constricting rock matrix led to an increase in the local capillary trapping, a trapping mechanism resulting from intrinsic capillary heterogeneity (Saadatpoor *et al.*, 2010). This was duly represented by the P_c–S relationships in the model and explains why the impact of the static parameter on capillary trapping is not noticeable for the gradational changes investigated. Retention of CO_2 within the pore spaces is enhanced by the capillary forces acting at the pore throats. Due to the larger distribution of the capillary processes, graded bedding in the reservoir accounted for a higher degree of capillary trapping when the static and dynamic parameters were integrated. Normally graded reservoirs were seen to residually trap more CO_2 than their inversely graded counterparts. This was attributed to the gradual rise in the magnitude of capillary forces acting within normally graded stratum, as opposed to the fall in magnitude for the inversely graded stratum. Fig. 7 shows the quantification of CO_2 trapping for all cases modelled in Aquifer-1:

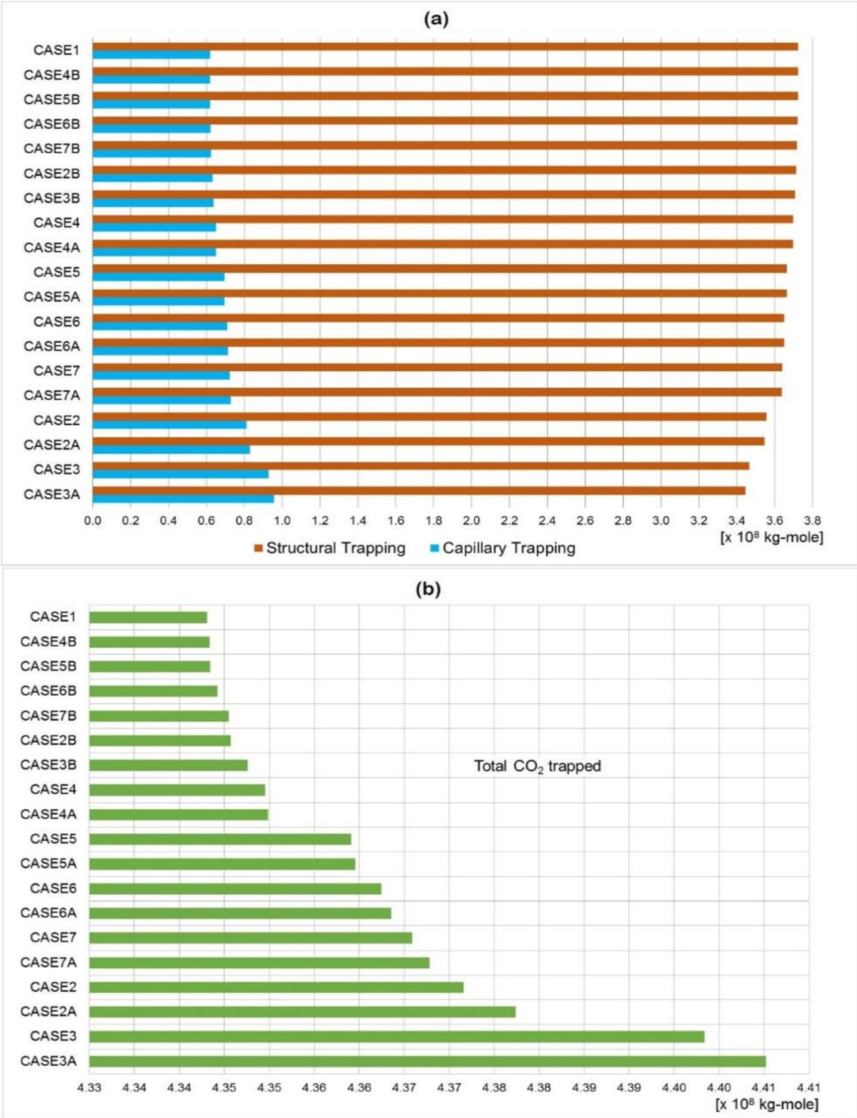

Fig. 7: a) Quantification of the physical trapping mechanisms and b) the total CO_2 trapped, in order of increasing total trapping from top to bottom, at the end of the injection period.

We observe in Fig. 7a that more gas is trapped residually as we proceed from the top, Case 1, to the bottom, Case 3A, of the chart. The prominence of capillary trapping within the reservoir serves to reduce the rate of CO_2 spreading at the base of the caprock, as well as increasing brine contact which is beneficial for CO_2 dissolution (Golding *et al.*, 2011). This was noted through the lateral extent of plume migration beneath the caprock for all simulated cases which followed the trend 1 > 4 > 2> 5 > 6 > 7 > 3 in the order Phase III > Phase I > Phase II. It suggests that the failure to include a variance in the P_c–S–k_r functions within the reservoir domain will lead to an over estimation of bouyant drive to- and the gravity current at- the transition zone. Following this observation, the open aquifer, i.e. Aquifer-2, became only an extension of Phase II for an analysis on overpressure.

ACCEPTED MANUSCRIPT

4.3 Pressure Evolution

To simulate the pressure evolution in the reservoir we first assumed an infinite lateral communication at both ends of the modelled domain. This was undertaken to identify which of the cases of gradational contact at the transition zone and gradation in the reservoir would have the least impact on the structural integrity of the caprock. The assumption of an infinite-acting aquifer was reasonably based on the vast lateral extent of the Bunter sandstone rock unit which crops up onshore in Eastern England as the Sherwood Sandstone Group (Brook *et al.*, 2003). To assess the structural trapping mechanism, we quantified the volume of mobile CO_2 lodged at the transition zone after 20 years of CO_2 injection (Fig. 8).

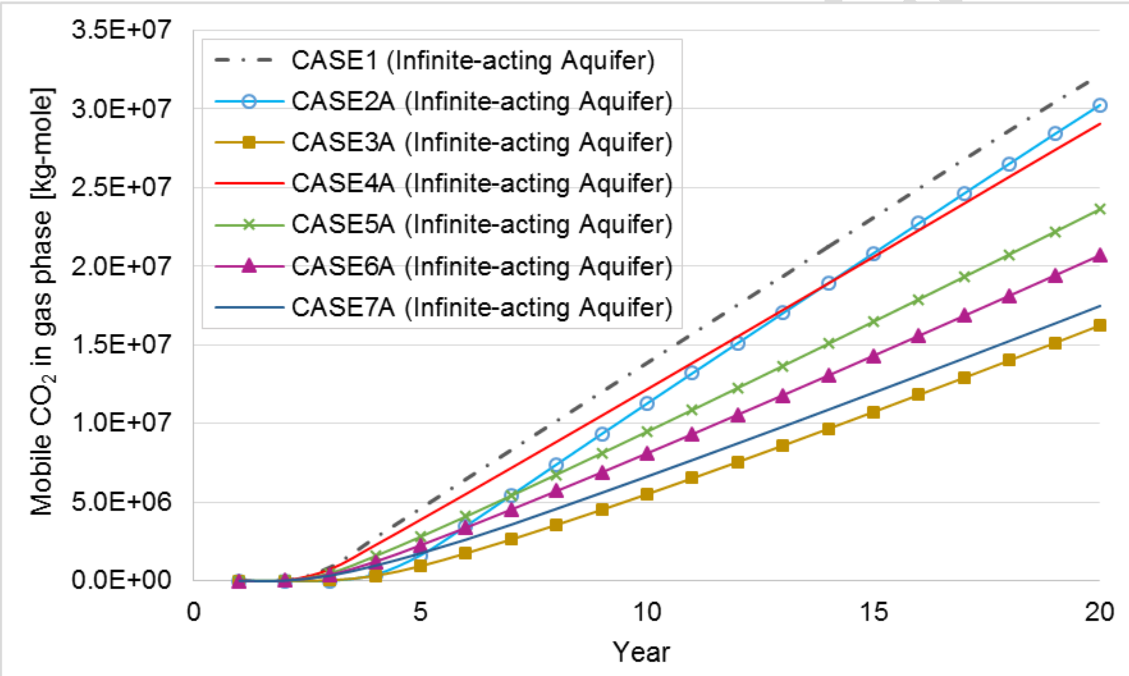

Fig. 8: Mobile CO_2 in the reservoir-seal gradation zone of an aquifer with infinite lateral communication.

As illustrated in section 4.2, the proportion of mobile CO_2 at the transition zone is influenced by the average particle-size within the rock matrix. This can be seen in a comparison between Case 3A and 2A where a decreasing particle-size, from the base to the top of Case 3A aquifer, progressively reduced the amount of free gas migrating vertically. On the other hand, the increasing particle-size from the base to the top of Case 2A propelled the vertical migration of CO_2 plume. Following the observations in Fig. 7, Case 3A and 7A were chosen for respective analysis on the impact of a graded reservoir and a gradational contact at the reservoir-seal interface on the pressure distribution in the domain. These cases showed the lowest magnitude of buoyant force in the transition zone. Consequently, Case 1, 3A, and 7A were simulated in a version of Aquifer-2 that reflected the probable pore volume of the Bunter Sandstone Formation (Table 6).

Reservoir Formation Domain	**Reservoir Pore Volume (rm^3)**	**Reference**
Aquifer-2 (Infinite-acting)	4.83E+14	Current study
Aquifer-2 (Bunter-estimation)	1.45E+12	Current study
Bunter Sandstone	1.52E+12	(Brook *et al.*, 2003)
Bunter Sandstone	1.396 E+12	(Holloway *et al.*, 2006)

Table 6: Provisional figures for reservoir pore volume used in this study

In the Bunter-estimate version of Aquifer-2, overpressure in the transition zone varied directly with the mass of free CO_2 in the strata. However, pressure evolution in the overlying caprock did not show such correlation (Fig 9):

ACCEPTED MANUSCRIPT

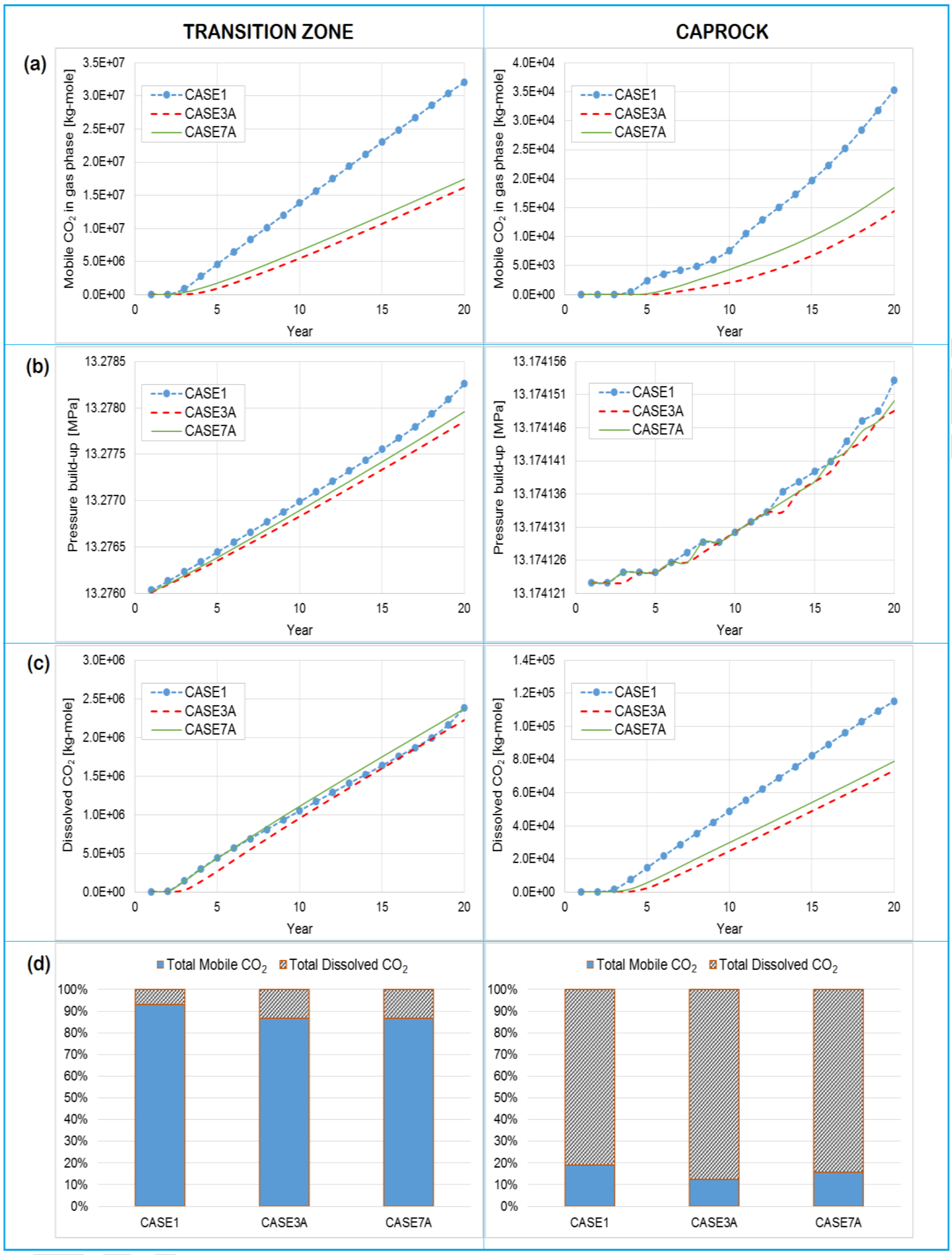

Fig. 9: Time plots showing: a) mobile CO_2, b) pressure evolution, and c) CO_2 dissolution through the injection period; as well as d) the percentage volume of total dissolved and mobile CO_2 at the 20th year of injection, in the transition zone and the caprock respectively.

This disparity was accounted for by the measure of capillary trapped CO_2 within each strata. This is because in pore spaces, the incumbent aqueous phase will further dissolve immobilised CO_2 ganglia which can account for the pressure drop (Peters *et al.*, 2015). In other words, the degree of CO_2 dissolution through residual trapping within a strata serves to counteract the impact of mobile CO_2 saturation on the pore fluid pressure (Fig. 9d). Notwithstanding, the results suggest that pore pressure within caprocks superjacent to graded strata at the reservoir/seal interface will show a lower evolution profile in comparison to those that are further removed. This assumption, however, is mostly valid for a field-scale determination of pressure evolution within the caprock. Generally, higher capillary forces resulting from smaller pore geometry tend to thicken the horizontal gravity current as a result of the reduced effective permeability of the intruding CO_2 (Fig. 10):

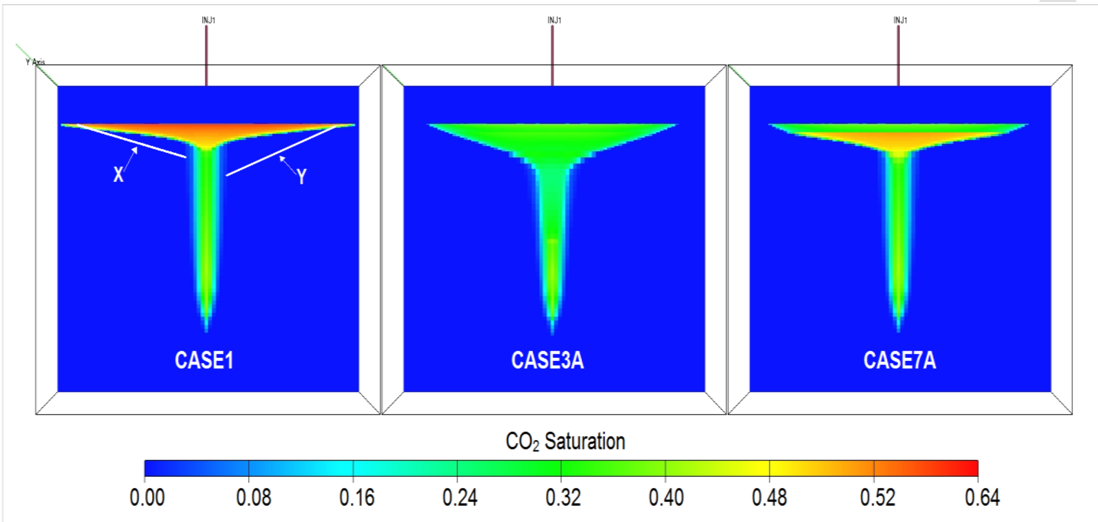

Fig. 10: A depiction of CO_2 saturation in the 20th year of gas injection. NB: The curves X and Y in Case1 illustrate the trend for gravity current in Case7A and Case3A respectively.

This usually results in a larger capillary fringe, i.e the region occupied by both phases. With constant CO_2 flux, the partial saturation of the non-wetting phase within the capillary fringe increases and thicker horizontal currents contact a greater region of the reservoir (Golding *et al.*, 2013). This has an immediate effect on pressure evolution within the contact area, as localised pore pressures increase while the capillary forces within the matrix immobilise the CO_2 ganglia. This phenomenon was notably observed around the injection well within the reservoir and the caprock at the end of the numerical simulation (Fig. 11):

ACCEPTED MANUSCRIPT

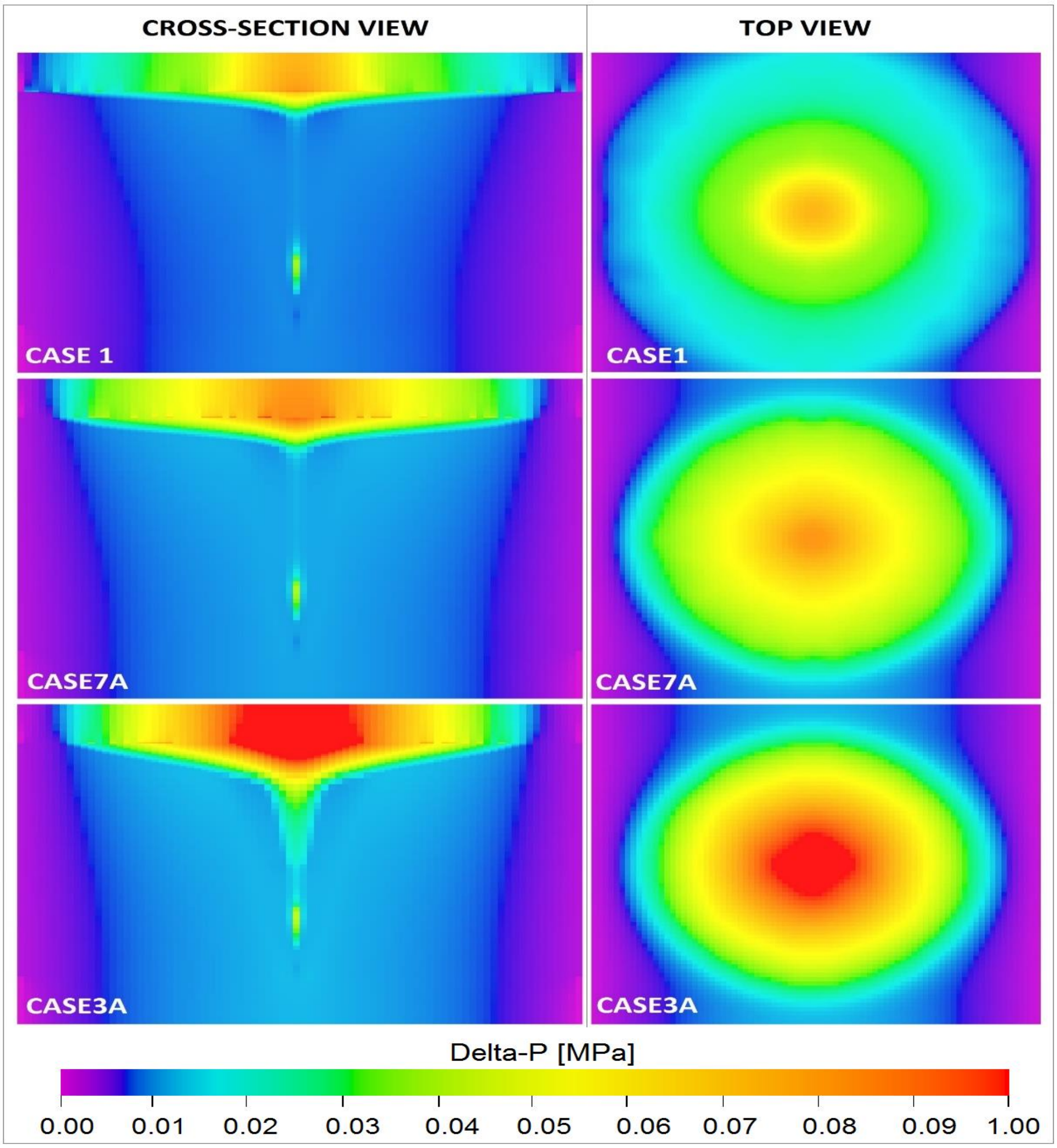

Fig. 11: 2D illustration of pressure change in the 20th year of CO_2 injection.

The reasoning is that within a thinning pore matrix, higher capillary forces correlate to a higher saturation of irreducible brine. The lateral continuity of such a matrix will result in little or no path being available for the migrating CO_2 plume to bypass the constricted strata, hence the gravity current expands beneath it. A consequence is the increased local capillary trapping of the gas within the strata, while the continous flux of the buoyant CO_2 plume results in CO_2 permeability though the region of highest gas concentration. The significance of a laterally continous reservoir-seal gradation zone within a semi-finite aquifer is a higher overpressure around the injection point, thus increasing the magnitude of pressure transmitted in the lower part of the caprock.

5 Summary and Conclusions

Numerical modelling of CO_2 geosequestration is to a large extent dependent on the quality of the quantitative knowledge of the geological descriptions that is used in the construction of the reservoir model. Through relating fluid and transport processes to primary sedimentary structures in siliciclastic formations, we employed numerical simulation to probe the heterogeneic effects of dynamic flow parameters on CO_2 storage performance. The results emphasise the significance of enhancing geological details in reservoir-specific models. Specifically, we identified the importance of modelling heterogeneity in the capillary pressure and relative permeability functions. We have demonsrated that for CO_2 storage in geological formations, the reservoir injectivity and trapping mechanisms are sensitive to gradational changes at the reservoir-seal interface as well as within the reservoir. Clast-size gradation from coarser- to finer- sediments within the reservoir leads to more favorable capillary trapping scenarios for CO_2 sequestration, irrespective of the boundary conditions. Gradation further increases the opportunity for CO_2 dissolution during the injection phase. Hence, the presence of these structures is vital in numerical models that investigate the post-injection sequestration processes. We also showed that the measure of how such sedimentary structures influence CO_2 storage will not be adequately determined if their description is based on the permeability and porosity data alone. This is based on the observation that the relative permeability data essentially dictates the effective permeability of fluids in a porous media.

The presence of a gradational contact at the reservoir-seal interface can also impact on the storage security. The study showed that for an open aquifer, the lateral continuity of such structures will likely reduce the field-scale overpressure in the caprock by mitigating brine migration into the seal. However, this could also increase localised pore pressures centred on the injection point within the caprock. Such scenarios can lead to the hydraulic fracturing of structural traps within the injection point, especially at the base of the trapping unit (Rozhko *et al.*, 2007). Gradation at the reservoir-seal interface may then be said to improve field-scale CO_2 storage security while also diminishing local-scale caprock integrity. This creates a paradoxical impact of gradation on structural trap integrity and further goes to highlight the importance of including such geological detail in numerical simulation studies.

ACCEPTED MANUSCRIPT

In summary, we conclude that numerical models which disregard the sensitivity of geological detail to multi-phase fluid transport processes will fail to sufficiently account for CO_2 storage performance. This is specifically with respect to various P_c–S–k_r relationships that may arise from the variance in pore geometry. We acknowledge that the present results were obtained under the simplifying assumption that variations in these constitutive functions only depend on the average grain size. There is room for further investigation by considering the effects of additional factors such as cemented sand layers, impermeable faults, leaky well bores, etc. on changes in hydraulic properties. For instance, faults are important in compartmentalising reservoirs and modifying the depositional continuity (Bouvier *et al.*, 1989). The increased knowledge of fault-induced reservoir compartmentalisation and communication can influence how primary sedimentary structures define reservoir flow processes. Also, subsequent diagenetically precipitated materials post particle deposition can form tightly cemented flow barriers within the reservoir. Laterally continous cementation not only constitutes barriers to flow but may also form pressure seals which can impact on the reservoir injectivity (Bjørkum and Walderhaug 1990). Hence, detailed sedimentary and petrographic analyses, including the fine-scale examination of well data and reservoir-specific models, are required to adequately predict CO_2 storage performance. Our future work will include other sedimentary features including faults with different transmissibility and cemented sand in the model in order to study their influence on the results.

Acknowledgments

This material is based upon work supported by Coventry University's Flow Measurement and Fluid Mechanics Research Centre. The authors would like to thank Schlumberger for the use of ECLIPSE and Petrel Software. We appreciate the constructive input of Dr. Adrian Wood and Dr. Philip Costen, including valuable comments from three anonymous reviewers.

ACCEPTED MANUSCRIPT

References

Al-khdheeawi, E.A., Vialle, S., Barifcani, A. et al. 2017. Impact of reservoir wettability and heterogeneity on CO_2 plume migration and trapping capacity. *International Journal of Greenhouse Gas Control* **58**: 142-158.

Bachu, S. 2015. Review of CO_2 storage efficiency in deep saline aquifers. *International Journal of Greenhouse Gas Control* **40**: 188-202.

Bear, J. 1972. *Dynamics of Fluids in Porous Media*. New York: American Elsevier Publishing Company.

Bennion, D.B. and Bachu, S. 2008. Drainage and imbibition relative permeability relationships for supercritical CO_2/brine and H_2S/brine systems in intergranular sandstone, carbonate, shale, and anhydrite rocks. *SPE Reservoir Evaluation and Engineering* **11**: 487-96.

Benson, S.M. and Cole, D.R. 2008. CO_2 Sequestration in Deep Sedimentary Formations. *Elements* **4** (5): 325-31. doi: 10.2113/gselements.4.5.325.

Benton, M.J., Cook, E. and Turner, P. 2002. *Permian and Triassic Red Beds and the Penarth Group of Great Britain*, Geological Conservation Review Series, No. 24 edition. Peterborough: Joint Nature Conservation Committee.

Bigelow, E.L. 1992. *Introduction to Wireline Log Analysis*. Texas: Western Atlas International.

Birkholzer, J.T., Zhou, Q. and Tsang, C. 2009. Large-scale impact of CO_2 storage in deep saline aquifers: A sensitivity study on pressure response in stratified systems. *International Journal of Greenhouse Gas Control* **3** (2): 181-94.

Bjørkum, P.A., and Walderhaug, O. 1990. Lateral extents of calcite-cemented zones in shallow marine sandstones. In *North Sea Oil and Gas Reservoirs – II*, ed. A. T. Buller, E. Berg, O. Hjelmeland et al., pp. 331-336. London: Graham and Trotman.

Bjørlykke, K. 2010. *Petroleum Geoscience: From Sedimentary Environments to Rock Physics*. Berlin: Sringer-Verlag.

Bloomfield, J.P., Gooddy, D.C., Bright, M.I. et al. 2001. Pore-throat size distributions in Permo-Triassic sandstones from the United Kingdom and some implications for contaminant hydrogeology. *Hydrogeology Journal* **9** (3): 219-30.

Boggs, S. 2009. *Petrology of sedimentary rocks*, 2nd edition. Cambridge: Cambridge University Press.

Bondor, P.L. 1992. Applications of carbon dioxide in enhanced oil recovery. *Energy Conversion and Management* **33** (5): 579-86.

Bouvier, J.D., Kaars-Sijpesteijn, C.H., Kluesner, D.F. et al. 1989: Three-dimensional seismic interpretation and fault sealing investigations, Nun River Field, Nigeria. *AAPG Bulletin* **73** (11): 1397-1414.

Brook, M., Shaw, K., Vincent, C. et al. 2003. Storage potential of the Bunter Sandstone in the UK sector of the Southern North Sea and the adjacent onshore area of eastern England. **CR/03/154**.

Brooks, R.H. and Corey, A.T. 1966. Properties of Porous Media Affecting Fluid Flow. *Journal of the Irrigation and Drainage Division* **92** (2): 61-90.

Burton, M., Kumar, N. and Bryant, S.L. 2009. CO_2 injectivity into brine aquifers: Why relative permeability matters as much as absolute permeability. *Energy Procedia* **1** (1): 3091-8.

Cameron, D.A. and Dyrlofsky, L.J. 2012. Optimization of well placement, CO_2 injection rates, and brine cycling for geological carbon. *International Journal of Greenhouse Gas Control* **10**: 100-112.

Carsel, R.F., Parrish, R.S. 1988. Developing joint probability distributions of soil water retention characteristics. *Water Resources Research* **24** (5): 755-769.

Chiquet, P., Daridon, J., Broseta, D. et al. 2007. CO_2/water interfacial tensions under pressure and temperature conditions of CO_2 geological storage. *Energy Conversion and Management* **48** (3): 736-44.

ACCEPTED MANUSCRIPT

Class, H., Edigbo, A., Helmog, R. et al. 2009. A benchmark study on problems related to CO_2 storage in geologic formations. *Computational Geosciences* **13** (4): 409.
Corey, A.T. 1954. The interellation between gas and oil relative permeabilites. *Producers Monthly* **19**: 38-41.
Darling, T. 2005. *Well Logging and Formation Evaluation*. Houston, Texas: Elsevier, Gulf Professional Publishing.
Dempsey, D., Kelkar, S., Pawar, R. et al. 2014. Modeling caprock bending stresses and their potential for induced seismicity during CO_2 injection. *International Journal of Greenhouse Gas Control* **22**: 223-36.
Doughty, C. and Pruess, K. 2004. Modeling supercritical carbon dioxide injection in heterogeneous porous media. *Vadose Zone Journal* **3**: 837-47.
Doveton, J.H. 1991. Lithofacies and Geochernical-*Facies Profiles* from Modern *Wireline Logs* - New Subsurface Templates for Sedimentary Modeling. In *Sedimentary Modelling: Computer Simulations and methods for improved parameter definition*, ed. E.K. Franseen, W.L. Watney, C.G. St. Kendall et al., pp. 101-110. Kansas: Kansas Geological Survey Bulletin 233.
Elewaut, E., Koelewijin, D., van der Straaten, R. et al. 1996. Inventory of the theoretical CO_2 storage capacity of the European Union and Norway. In *The Underground Disposal of Carbon Dioxide. Final Report of Joule II Project No. CT92-0031*, ed. S. Holloway, pp. 16-115. Keyworth, Nottingham: British Geological Survey.
Ennis-King, J.P. and Paterson, L. 2005. Role of Convective Mixing in the Long-Term Storage of Carbon Dioxide in Deep Saline Formations. *SPE Journal* **10** (03): 349-56.
Espinet, A., Shoemaker, C. and Doughty, C. 2013. Estimation of plume distribution for carbon sequestration using parameter estimation with limited monitoring data. *Water Resources Research* **49** (7): 4442-4464.
Fabricius, I.L., Fazladic, L.D., Steinholm, A. et al. 2003. The use of spectral natural gamma-ray analysis in reservoir evaluation of siliciclastic sediments: a case study from the Middle Jurassic of the Harald Field, Danish Central Graben. *Geological Survey of Denmark and Greenland Bulletin* **1**: 349-66.
Fleet, M., Gurton, R. and Taggart, I. 2004. The Function of Gas-Water Relative Permeability Hysteresis in the Sequestration of Carbon Dioxide in Saline Formations. Presented at the SPE Asia Pacific Oil and Gas Conference and Exhibition, Perth, Australia, 18-20 October.
Folk, R.L. 1974. *The Petrology of Sedimentary Rocks*. Texas: Hemphill Publishing Company.
Golding, M.J., Huppert, H.E. and Neufeld, J.A. 2013. The effects of capillary forces on the axisymmetric propagation of two-phase, constant-flux gravity currents in porous media. *Physics of Fluids* **25** (3): 036602. doi: 10.1063/1.4793748.
Golding, M.J., Neufeld, J.A., Hesse, M.A. et al. 2011. Two-phase gravity currents in porous media. *Journal of Fluid Mechanics* **678**: 248-70. doi: 10.1017/jfm.2011.110.
Gor, G.Y., Elliot, T.R. and Prevost, J.H. 2013. Effects of thermal stresses on caprock integrity during CO_2 storage. *International Journal of Greenhouse Gas Control* **12**: 300-309.
Gozalpour, F., Ren, S.R. and Tohidi, B. 2005. CO_2 EOR and Storage in Oil Reservoir. *Oil & Gas Science and Technology - Rev.IFP* **60** (3): 537-46.
Grigg, R.B. 2005. Long-Term CO_2 Storage: Using Petroleum Industry Experience. In *Carbon Dioxide Capture for Storage in Deep Geologic Formations*, ed. D.C. Thomas, pp. 853-865. Amsterdam: Elsevier Science.
Hebach, A., Oberhof, A., Dahmen, N. et al. 2002. Interfacial Tension at Elevated Pressures-Measurements and Correlations in the Water + Carbon Dioxide System. *Journal of Chemical & Engineering Data* **47** (6): 1540-6.
Hiscott, R.N. 2003. Grading, graded bedding. In *Sedimentology*, Chap. 535-538. Dordrecht: Springer Netherlands.
Haldorsen, H.H. 1986. Simulation parameter assignment and the problem of scale in reservoir engineering. In *Reservoir Characterisation*, ed. L.W. Lake and H.B. Carroll, Jr., pp. 293-340. London: Academic Press.

ACCEPTED MANUSCRIPT

Holloway, S., Vincent, C.J., Bentham, M.S. et al. 2006. Top-down and bottom-up estimates of CO_2 storage capacity in the United Kingdom sector of the southern North Sea basin. *Environmental Geosciences* **13** (2): 71-84. doi: 10.1306/eg.11080505015.

IPCC 2005. IPCC Special Report on Carbon Dioxide Capture and Storage. Prepared by Working Group III of the Intergovernmental Panel on Climate Change.

James, A., Baines, S. and McCollough, S. 2016. D10: WP5A – Bunter Storage Development Plan. **10113ETIS-Rep-13-03**: 1-212.

Juanes, R., Spiteri, E.J., Orr, F.M. et al. 2006. Impact of relative permeability hysteresis on geological CO_2 storage. *Water Resources Research* **42** (12): W12418.

Katahara, K.W. 1995. Gamma Ray Log Response in Shaly Sands. *The Log Analyst* **36** (4): 50-71.

Kopp, A., Class, H. and Helmig, R. 2009. Investigations on CO_2 storage capacity in saline aquifers. *International Journal of Greenhouse Gas Control* **3** (3): 263-76.

Kovscek, A.R. and Cakici, M.D. 2005. Geologic storage of carbon dioxide and enhanced oil recovery. II. Cooptimization of storage and recovery. *Energy Conversion and Management* **46** (11): 1941-56.

Krevor, S., Blunt, M.J., Benson, S.M. et al. 2015. Capillary trapping for geologic carbon dioxide storage – From pore scale physics to field scale implications. International Journal of Greenhouse Gas Control **40**: 221-237.

Kumar, A., Ozah, R., Noh, M. et al. 2005. Reservoir Simulation of CO_2 Storage in Aquifers. *SPE Journal* **10** (03): 336-48.

Lawter, A.R., Qafoku, N.P., Asmussen, R.M. et al. 2017. Risk of Geologic Sequestration of CO_2 to Groundwater Aquifers: Current Knowledge and Remaining Questions. *Energy Procedia* **114** (Supplement C): 3052-9.

Martin, D.F. and Taber, J.J. 1992. Carbon Dioxide Flooding. *Journal of Petroleum Technology* **44** (04): 396-400.

Meckel, T.A., Bryant, S.L., Ganesh, P.R., 2015. Characterization and prediction of CO_2 saturation resulting from modelling buoyant fluid migration in 2D heterogeneous geologic fabrics. International Journal of Greenhouse Gas Control **34**: 85–96.

Mo, S., Zweigel, P., Lindeberg, E. et al. 2005. Effect of Geologic Parameters on CO_2 Storage in Deep Saline Aquifers. Presented at the SPE Europec/EAGE Annual Conference, Madrid, Spain, 13-16 June.

Mori, H., Trevisan, L. and Illangasekare, T.H. 2015. Evaluation of relative permeability functions as inputs to multiphase flow models simulating supercritical CO_2 behavior in deep geologic formations. *International Journal of Greenhouse Gas Control* **41**: 328-335.

Mualem, Y. 1976. A new model for predicting the hydraulic conductivity of unsaturated porous media. *Water Resources Research* **12** (3): 513-22.

Nazeer, A., Abbasi, S.A. and Solangi, S.H. 2016. Sedimentary facies interpretation of Gamma Ray (GR) log as basic well logs in Central and Lower Indus Basin of Pakistan. *Geodesy and Geodynamics* **7** (6): 432-43.

Newell, A. and Shariatipour, S.M. 2016. Linking outcrop analogue with flow simulation to reduce uncertainty in sub-surface carbon capture and storage: an example from the Sherwood Sandstone Group of the Wessex Basin, UK. In *The value of outcrop studies in reducing subsurface uncertainty and risk in hydrocarbon exploration and production*, ed. M. Bowman, H.R. Smyth, T.R. Good et al., pp. 231-246. London: Geological Society Special Publications 436.

Newell, A.J. 2017. Evolving stratigraphy of a Middle Triassic fluvial-dominated sheet sandstone: The Otter Sandstone Formation of the Wessex Basin (UK). *Geological Journal*: 1-19.

Nicol, A., Carne, R., Gerstenberger, M. et al. 2011. Induced seismicity and its implications for CO_2 storage risk. *Energy Procedia* **4** (Supplement C): 3699-706.

Noy, D.J., Holloway, S., Chadwick, R.A. et al. 2012. Modelling large-scale carbon dioxide injection into the Bunter Sandstone in the UK Southern North Sea. *International Journal of Greenhouse Gas Control* **9**: 220-33.

ACCEPTED MANUSCRIPT

Obi, E.I. and Blunt, M.J. 2006. Streamline-based simulation of carbon dioxide storage in a North Sea aquifer. *Water Resources Research* **42**, (3): 1-13. doi: 10.1029/2004WR003347.

Oldenburg, C.M., Pruess, K. and Benson, S.M. 2001. Process modeling of CO_2 injection into natural gas reservoirs for carbon sequestration and enhanced gas recovery. *Energy Fuels* **15** (2): 293-298.

Oostrom, M., White, M.D., Porse, S.L. et al. 2016. Comparison of relative permeability–saturation–capillary pressure models for simulation of reservoir CO_2 injection. *International Journal of Greenhouse Gas Control* **45**: 70-85.

Perrin, J. and Benson, S. 2010. An Experimental Study on the Influence of Sub-Core Scale Heterogeneities on CO_2 Distribution in Reservoir Rocks. *Transport in Porous Media* **82** (1): 93-109. doi: 10.1007/s11242-009-9426-x.

Peters, E., Egberts, P.J.P., Loeve, D. et al. 2015. CO_2 dissolution and its impact on reservoir pressure behavior. *International Journal of Greenhouse Gas Control* **43**: 115-23.

Pettijohn, F.J. 1957. *Sedimentary rocks*. 2nd Edn. New York: Harper.

Pettijohn, F.J., Potter, P.E. and Siever, R. 1972. *Sand and sandstones*. New York: Springer-Verlag.

Pruess, K., Xu, T., Apps, J. et al. 2003. Numerical Modeling of Aquifer Disposal of CO_2. *SPE Journal* **8** (01): 49-60.

Pruess, K. and Nordbotten, J. 2011. Numerical Simulation Studies of the Long-term Evolution of a CO_2 Plume in a Saline Aquifer with a Sloping Caprock. *Transport in Porous Media* **90** (1): 135-51. doi: 10.1007/s11242-011-9729-6.

Rhys, G.H. 1974. A proposed standard lithostratigraphic nomenclature for the southern North Sea and an outline structural nomenclature for the whole of the (UK) North Sea.

Rozhko, A.Y., Podladchikov, Y.Y. and Renard, F. 2007. Failure patterns caused by localized rise in pore-fluid overpressure and effective strength of rocks. *Geophysical Research Letters* **34** (22): L22304. doi: 10.1029/2007GL031696.

Saadatpoor, E., Bryant, S.L. and Sepehrnoori, K. 2010. New Trapping Mechanism in Carbon Sequestration. *Transport in Porous Media* **82** (1): 3-17.

Schlumberger. 2015. ECLIPSE SimLauncher, Version 2015.2.0.0.

Schlumberger. 2016. Petrel E&P Software Platform, Version 2016.

Shariatipour, S.M., Pickup, G.E. and Mackay, E.J. 2014. The effect of aquifer/caprock interface on geological storage of CO_2. *Energy Procedia* **63**: 5544-5555.

Sharaitipour, S.M., Pickup, G.E. and Mackay, E.J. 2016. Simulations of CO_2 storage in aquifer models with top surface morphology and transition zones. *International Journal of Greenhouse Gas Control* **54** (1): 117-128.

Shell 2011. UK Carbon Capture and Storage Demonstration Competition. UKCCS-KT-S7.19-Shell-002, SCAL Report.

Spain, D.R. and Conrad, C.P. 1997. Quantitative analysis of top-seal capacity: offshore Netherlands, southern North Sea. *Geologie en Mijnbouw* **76** (3): 217-26.

USDA 1987. Soil Mechanics Level I, Module 3: USDA Textural Soil Classification.

Van De Graaff, W.J.E. and Ealey, P.J. 1989. Geological modelling for simulation studies. *AAPG Bulletin* **73** (11): 1436-1444

Van Genuchten, M.T. 1980. A Closed Form Equation for Predicting the Hydraulic Conductivity of Unsaturated Soils. *Soil Science Society of America Journal* **44**: 892-8.

Wentworth, C.K. 1922. A Scale of Grade and Class Terms for Clastic Sediments. *The Journal of geology* **30** (5): 377-92. doi: 10.1086/622910.

Williams, J.D.O., Jin, M., Bentham, M. et al. 2013. Modelling carbon dioxide storage within closed structures in the UK Bunter Sandstone Formation. *International Journal of Greenhouse Gas Control* **18**: 38-50.

Zheng, L., Spycher, N., Birkholzer, J. et al. 2013. On modeling the potential impacts of CO_2 sequestration on shallow groundwater: Transport of organics and co-injected H_2S by supercritical CO_2 to shallow aquifers. *International Journal of Greenhouse Gas Control* **14**: 113-27.

ACCEPTED MANUSCRIPT

Zhou, Q., Birkholzer, J.T., Mehnert, E. et al. 2010. Modeling basin- and plume-scale processes of CO_2 storage for full scale deployment. *Ground Water* **48** (4): 494-514.

ACCEPTED MANUSCRIPT